communications
earth & environment

ARTICLE

https://doi.org/10.1038/s43247-023-00889-0 OPEN

Irrigation benefits outweigh costs in more US croplands by mid-century

Trevor Partridge [1,2✉], Jonathan Winter [1,3], Anthony Kendall [4], Bruno Basso [4,5], Lisi Pei[4,6] & David Hyndman [7]

Irrigation can increase crop yields and could be a key climate adaptation strategy. However, future water availability is uncertain. Here we explore the economic costs and benefits of existing and expanded irrigation of maize and soybean throughout the United States. We examine both middle and end of the 21st-century conditions under future climates that span the range of projections. By mid-century we find an expansion in the area where the benefits of irrigation outweigh groundwater pumping and equipment ownership costs. Increased crop water demands limit the region where maize could be sustainably irrigated, but sustainably irrigated soybean is likely feasible throughout regions of the midwestern and southeastern United States. Shifting incentives for installing and maintaining irrigation equipment could place additional challenges on resource availability. It will be important for decision makers to understand and account for local water demand and availability when developing policies guiding irrigation installation and use.

[1] Department of Earth Sciences, Dartmouth College, Hanover, NH, USA. [2] U.S. Geological Survey, Water Resources Mission Area, Lakewood, CO, USA. [3] Department of Geography, Dartmouth College, Hanover, NH, USA. [4] Department of Earth and Environmental Sciences, Michigan State University, East Lansing, MI, USA. [5] W.K. Kellogg Biological Station, Michigan State University, Hickory Corners, MI, USA. [6] Georgia Institute of Technology, School of Civil and Environmental Engineering, Atlanta, GA, USA. [7] Department of Geosciences, The University of Texas at Dallas, Richardson, TX, USA.
✉email: tpartridge@usgs.gov

In the coming decades, annual temperatures in the United States are projected to rise by an additional 1.4 °C regardless of the future emission trajectory[1], and global food demand is expected to increase from 35% to 56%[2–4]. Agriculture is one of the most vulnerable sectors to climate change and observed warming has already led to reduced agricultural yields[5,6]. To ensure food security while minimizing adverse environmental impacts, it is necessary to understand the potential effects of climate change on agricultural productivity and critically examine adaptation strategies, especially as some adaptations may be maladaptive for compound extreme events[7]. Expanding irrigated agriculture is often suggested as a promising management adaptation[8,9] that could help meet growing food demand[10–12] while making agriculture more resilient to drought. However, irrigated agriculture is already the single largest consumer of global freshwater resources. Historical irrigation has reduced environmental flows below critical levels in many regions[13,14], lead to the depletion of groundwater resources[15], and is itself a source of greenhouse gas emissions[16]. Continued unsustainable water use practices coupled with uncertain future water availability may limit the feasibility of irrigation as a climate adaptation strategy[17–22].

In the U.S., less than 20 percent of harvested cropland is equipped for irrigation, yet irrigated crops often account for more than half of total crop sales[23]. In recent decades, efficiency improvements have reduced total irrigated water use while irrigated area has increased, yet irrigated agriculture still accounts for roughly 80 percent of the country's water use[24]. Early integrated assessments examining future changes to regional water availability[25] and irrigation water demand[26] suggested that the total amount of irrigated water applied will likely decline as a result of either insufficient water resources or reduced demand. However, there is still considerable uncertainty around future water availability, irrigation requirements, and the response of marginal yields (i.e., the difference between irrigated and rainfed yield) to climate change scenarios with concurrent temperature and precipitation change[27,28]. For example, early studies found that historic productivity in the midwestern U.S. could be maintained with little to no additional irrigation, at least through mid-century[29,30]. More recent work has suggested that the region might require substantial increases in irrigation to meet future crop water demands[31,32], unless a historic anomalous cooling pattern persists[33,34]. Uncertainty in future irrigation requirements arises from both uncertainties surrounding future precipitation changes as well methodological differences between crop models and studies. Many projections that directly simulate the effect of changing precipitation on yield are coarse resolution or have simple representations of crop growth and irrigation practices (e.g., fixed scheduling). Updated climate projections from the sixth Climate Model Intercomparison Project (CMIP6), as well as recent advancements in physical crop models, such as growth stage deficit irrigation[35], will help reduce uncertainty in estimating future water resources and irrigated water demand[21].

While there are many environmental, institutional, technological, and equity challenges surrounding expanding irrigated agriculture, it's likely that irrigation will be a crucial component of meeting future food demand. Optimizing the value of continued and expanded irrigation in a changing climate demands a thorough understanding of the expected benefits (i.e., marginal yield gains) and costs (including capital, environmental, and social costs) across a range of plausible climate futures. Recent global analyses have improved our understanding of contemporary marginal yield gains from irrigation[28], quantified the present gross economic value of water used for irrigating a wide range of crops[36], and delineated areas where water resources could meet or exceed future crop water demand[21]. However, to the best of our knowledge, no study has yet projected the future value of water used for irrigation at a high resolution for the United States. Combining these projections with estimates of water availability is critical as it will help to identify areas where irrigation could be both profitable and sustainable.

Here we approximate the feasibility of expanded irrigation for maize (*Zea mays*) and soybean (*Glycine max*) at a 5-arcminute resolution over all cultivated areas in the U.S. through projecting two metrics: (I) the irrigation benefit to cost ratio ($Ir_{B/C}$) and (II) the irrigated water deficit. Crop model simulations are conducted using a gridded version of the Decision Support System for Agrotechnology Transfer model (pDSSAT)[37,38] for historical (1981–2010), mid-century (2036–2065) and end-of-century (2071–2100) conditions under moderate and high emissions trajectories from five statistically downscaled CMIP6 Global Climate Models (GCMs). The 5-model ensemble was selected as a representative sample of the range of future climates expected in the midwestern U.S.[39], with four GCMs representing one quadrant of future change in precipitation and temperature (i.e., hot & dry, hot & wet, cool & dry, cool & wet) and one representing the inter-model median (Supplementary Fig. 1 and Supplementary Table 1). Moderate and high emissions trajectories are exemplified by the paired Shared Socioeconomic Pathway (SSP) scenarios SSP245 and SSP585. SSPs are an important input for GCMs as they project global emissions as a function of plausible future socioeconomic scenarios and update the previously used Representative Concentration Pathways (RCPs) used in CMIP5[40]. Below we report results primarily from the five-member ensemble mean under a SSP245 emissions trajectory with SSP585 results included in the supplemental text.

Results

Projected changes in growing season climate. Average growing season temperatures in the midwestern U.S. could increase from 1.1 °C to 4.6 °C (1.9 °C to 8.8 °C) by the middle (end) of the 21st century, relative to historical averages from 1981–2010, depending on emissions trajectory and GCM (Fig. 1 and Supplementary Table 1). Precipitation changes in this region over the same period are less certain. Projected changes in growing season precipitation during the middle (end) of the century range from a 10.2% (12.3%) increase under climate projections from the NESM3 GCM[41] forced with SSP245 emissions (cool & wet scenario) to a 7.9% (16.9%) decrease under the HadGEM3 GCM[42] forced with SSP585 emissions (warm and dry scenario). The 5-GCM ensemble average under a SSP245 trajectory projects a moderate decrease in mid-century total growing season precipitation over much of the north-central U.S. with little change to a slight increase throughout parts of the Midwest and Mid-Atlantic regions (Fig. 1). A SSP585 emissions future is considerably drier than the lower emission trajectory, especially by the end of the 21st century (Supplementary Fig. 2). Average mid-century precipitation changes for each GCM are shown in Supplementary Figs. 3, 4.

Projected impacts on rainfed and irrigated crop yield. Historic crop cultivar parameters within pDSSAT were calibrated using crop progress data from the U.S. Department of Agriculture (USDA) National Agricultural Statistical Service (NASS)[23] (calibration process described in methods). Simulated historical maize and soybean yields reasonably approximate U.S. county average reported yields ($r^2 = 0.59$ and 0.57 respectively; Supplementary Fig. 5). Simulated yields can be modified through adjusting parameters controlling the planting density of crops as well as physiological parameters such as the number of grain kernels per plant and grain filling rates. We allow these parameters to evolve during the historical period to match yield trends but hold them

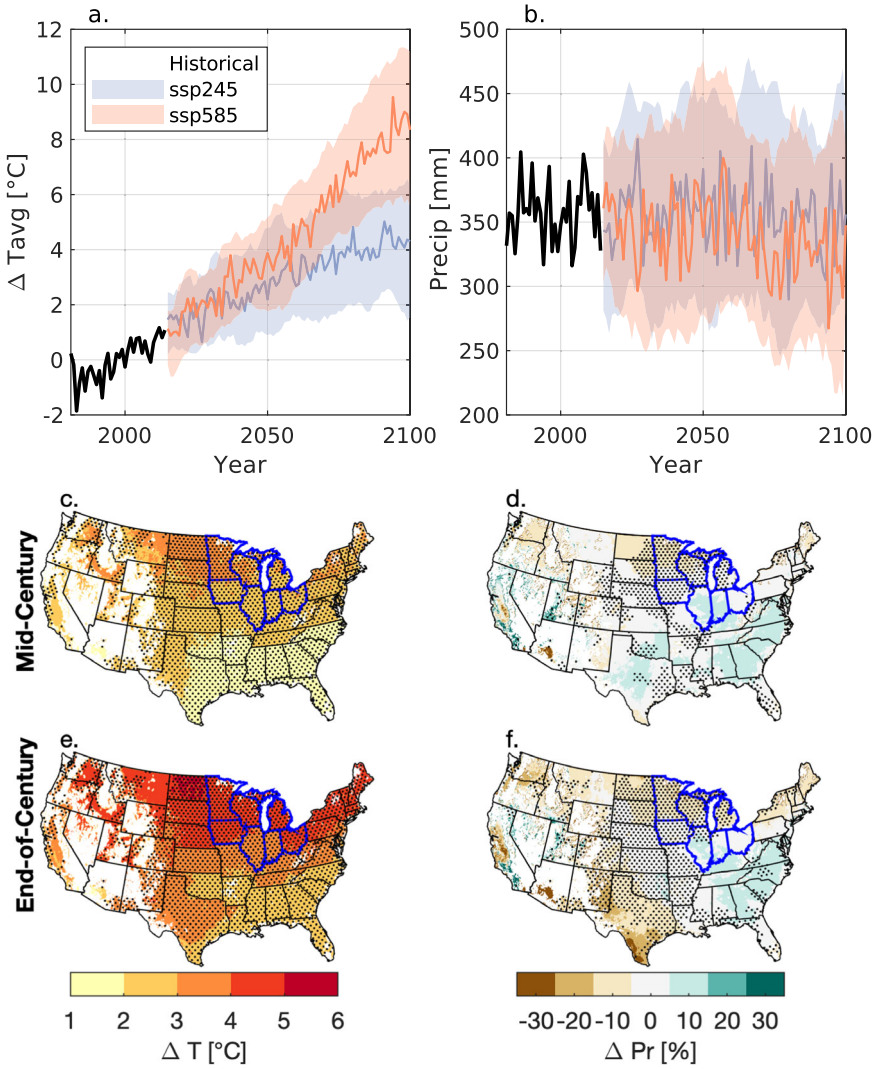

Fig. 1 Projected changes in growing season temperature and precipitation. Time series of June through September average temperature anomalies (**a**) and total precipitation (**b**) from the 5-member CMIP6 ensemble under moderate and high emissions future (SSP245 and SSP585 respectively) for the midwestern U.S., outlined in blue in maps. The solid line represents the inter-model mean and the shaded area is the smoothed ensemble range. **c**–**f** Ensemble mean change under a SSP245 trajectory in growing season average (not necessarily June through September) temperature (**c**, **e**) and total precipitation (**d**, **f**) by mid-century (2036–2065) and end of the century (2071–2100) over modeled grid cells. Stippling identifies areas where all GCMs agree on future change based on Kruskal–Wallis test. All changes are relative to historical (1981–2010) climatology.

fixed at contemporary values for future simulations. Farmers can relatively easily adapt to yearly fluctuations in growing season conditions through altering certain management decisions. We account for these adaptations through modifying future planting dates and maize cultivar selection based on future climate metrics. We do not modify soybean cultivars given the relatively broad temperature range of soybean maturity groups[43]. Future planting dates for maize and soybean were estimated by training a random forest model on observed planting dates and five early-season climate metrics (see methods). The trained model reasonably recreates observed planting dates ($r^2 = 0.88$ for the out-of-bag samples; Supplementary Fig. 6) and predicts little to no change in 30-year average planting date by mid-century and approximately a 1-week earlier planting date by the end of the century throughout most of the Midwest (Supplementary Fig. 7). For irrigated simulations, crops are automatically irrigated with 10 mm of water from an unlimited reservoir on days when plant available water falls below 40%. The average growing season applied water is shown in Supplementary Fig. 8 and closely approximates state level applied water data from the 2013 USDA Irrigation and Water Management Survey (maize $r^2 = 0.88$, soybean $r^2 = 0.81$; Supplementary Figs. 9 and 10).

Under a SSP245 emissions trajectory, model results show significant increases in mid-century irrigated and rainfed yields throughout most of the Corn Belt and eastern U.S., with small but significant decreases in parts of the southern High Plains (Fig. 2). We present both rainfed and irrigated yield for all simulated grid cells regardless of historic management. Historically rainfed and irrigated maize and soybean areas are shown in Supplementary Fig. 11 and analogous SSP585 yield maps are shown in Supplementary Fig. 12. Historic average simulated yields are shown in Supplementary Fig. 13. By the end of the century, we find significant decreases in rainfed and irrigated yields throughout the southern High Plains for maize, and to a lesser extent soybean, yet average yields in the Midwest remain higher than present. The SSP245 end-of-century yield maps largely resemble mid-century yield maps under a SSP585 future. A SSP585 emissions future could lead to substantial reductions in irrigated and rainfed maize throughout the majority U.S. by the end of the century. Future irrigated soybean yields remain higher than

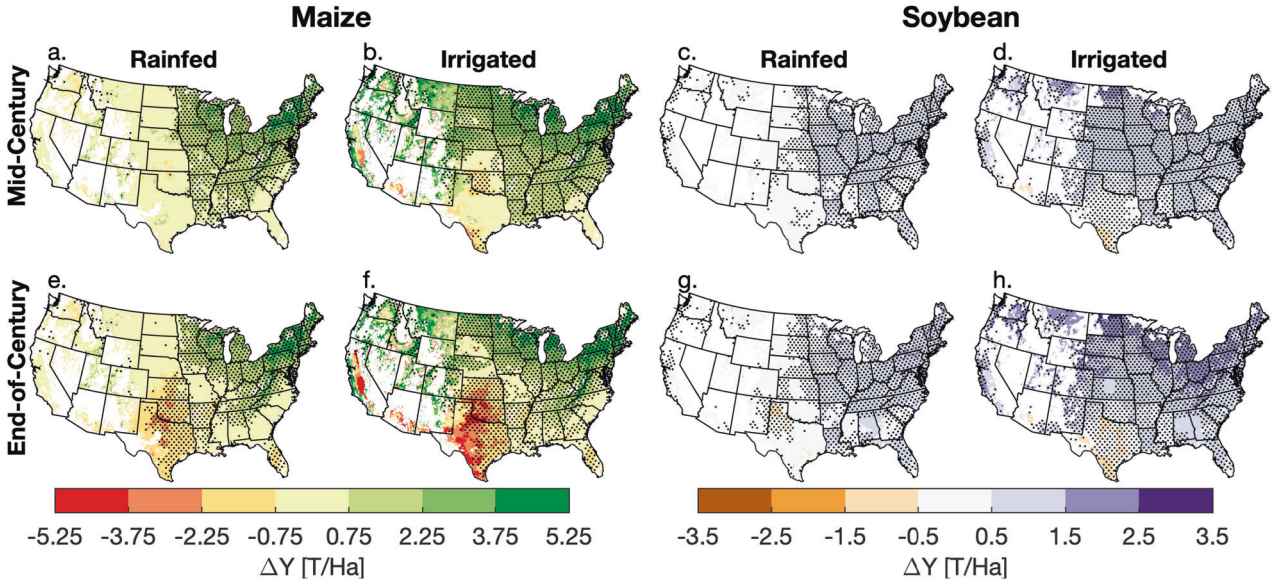

Fig. 2 Projected yield changes for Maize and Soybean. Change in ensemble average simulated yield under rainfed (**a**, **e**, **c**, **g**) and fully irrigated (**b**, **f**, **d**, **h**) conditions for maize and soybean under SSP245 mid-century (2036–2065) and end-of-century (2071–2100) climate. Changes are relative to corresponding average yield (i.e., rainfed or irrigated) from historical (1981–2010) simulations which are shown in Figs. S15 and S16. Stippling shows grid cells where full 5-GCM ensemble yield distribution is significantly different from historical yield distribution using Kolmogorov–Smirnov test.

present everywhere outside of the southern High Plains, Mississippi, and small regions in Georgia and South Carolina. It's important to note that GCMs have varying sensitivity that is reflected in both temperature and precipitation responses to changing greenhouse gas and other external forcings. Our future climate scenarios span a range of potential growing season conditions as illustrated by the timeseries in Fig. 1. The yield maps shown in Fig. 1 and Supplementary Fig. 12 represent the average expected response, for our given set of assumptions, under a particular emissions trajectory, not an assigned shift in temperature or precipitation (e.g., a 3 °C warmer world).

Recent work has found that farmers are not selecting for longer season maize cultivars[44] even though growing seasons have been increasing by roughly 1 day decade-1 since 1895[45]. Instead, farmers appear to select cultivars based on factors such as market forces, labor constraints, and field access[44]. We test the consequence of our assumption that farmers will shift to longer season maize cultivars through simulating the growth of historically grown maize cultivars under future climate conditions. In these supplemental simulations, we do allow for adaptive planting dates to account for interannual variability in early season conditions. Without cultivar adaptation, midcentury maize yields are still significantly higher than historical, though not as high as longer season cultivars, throughout the eastern and southeastern U.S. under a SSP245 (Supplementary Fig. 14) and, to a lesser extent, SSP585 (Supplementary Fig. 15) future. Throughout most of the Corn Belt, historically grown maize cultivar yields remain relatively static under a SSP245 midcentury climate and decrease slightly under SSP585. Planting historically grown maize cultivars during the end of the century could lead to average rainfed yield losses of 0.52–2.8 T Ha-1 throughout the Corn Belt depending on future emissions (Supplementary Figs. 14 and 15).

The marginal yield gain from irrigating historically ranges from less than 1 T Ha-1 in the eastern U.S. to greater than 10 T Ha-1 in the more arid western U.S. (Supplementary Fig. 16). The larger future increases in irrigated soybean yield relative to rainfed yield (Fig. 2) lead to a substantial increase in soybean marginal yield relative to the historical period. Future maize marginal yield also increases by mid-century throughout much of the western U.S., but the regions that show the greatest change in average marginal yield tend to be outside currently irrigated areas, including the north central U.S. and Michigan. In fact, currently, irrigated maize regions in Kansas and Oklahoma exhibit a minor decrease in average marginal yield by mid-century (Supplementary Fig. 17).

Irrigation economic returns. The economic return of irrigating depends on the value added from increasing marginal yields and the operational costs associated with irrigation infrastructure and use. As projected changes in future crop market and energy prices become unreliable after a few years, we hold crop and energy prices constant for future periods and report the economic benefit of irrigating as the irrigation benefit to cost ratio ($Ir_{B/C}$) for each grid cell and growing season. This assumes that crop and energy prices will fluctuate at roughly concurrent rates and that the modern ratio is a reasonable analog for the future. Briefly, the benefits of irrigating are calculated by multiplying the marginal yield gain by the 2000–2020 average international market price for maize and soybean ($160 and $365 Ton-1, respectively)[46]. Costs are approximated as a function of pumping costs and ownership costs. Pumping costs are approximated using regional energy prices[47] (Supplementary Fig. 18) and total depth to water after accounting for drawdown within the well and from the surrounding cone of depression from within season pumping[48]. Future groundwater availability will depend on withdrawal rates and climate. Due to the challenges associated with projecting future withdrawal rates, we hold future depth to groundwater at contemporary levels[49] for the start of each growing season. The variability in future pumping costs is a function of climate driven crop water requirements and the within growing season draw-down associated with pumping groundwater to meet those requirements. Ownership costs are estimated from available extension documents (Supplementary Table 2). We assume a central pivot system covering a ¼ mile field which is the most common irrigated field size in the U.S[50]. A detailed description of the $Ir_{B/C}$ calculation is included in the methods section and we discuss the implications of our assumptions in 'Discussion'. Values of $Ir_{B/C}$ can range from −1 to positive infinity, with 0 indicating a neutral benefit to cost. Despite our simplifying assumptions and the regional variability of pump, motor, and

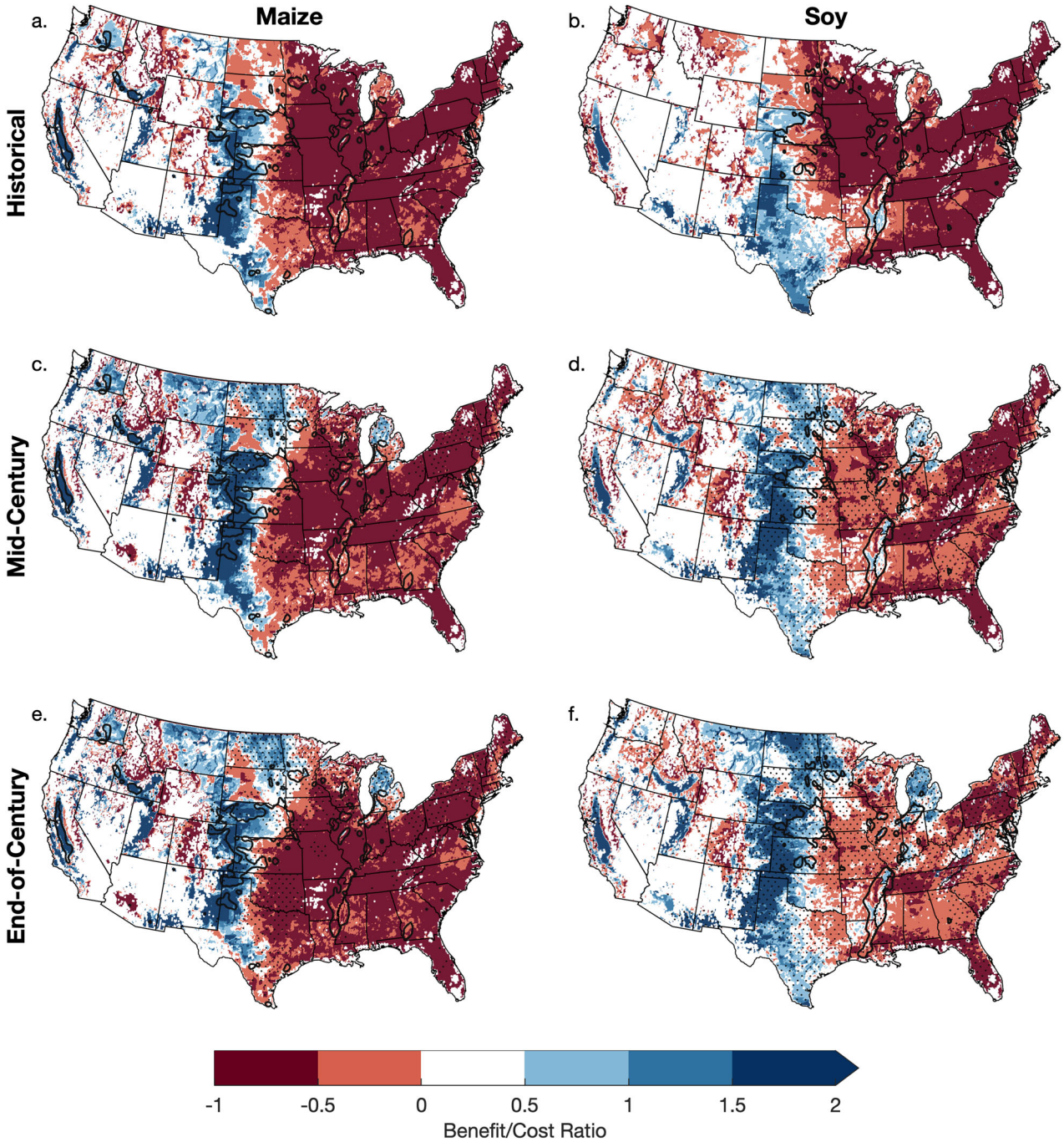

Fig. 3 Average 30-year irrigation benefit to cost ratio. 30-year average irrigation benefit to cost ratio for maize (**a**, **c**, **e**) and soybean (**b**, **d**, **f**) during the historical (1980–2010), mid-century (2036–2065) and end-of-century (2071–2100) time periods. Future time periods show a 5-GCM ensemble average under a SSP245 emissions trajectory. Stippling indicates grid cells with irrigation value distributions statistically different from historical distribution. Historical crop-specific irrigated areas are outlined in black.

application efficiencies, our estimates of irrigation costs reasonably approximate reported irrigation pumping costs from the 2013 Farm and Ranch Irrigation Survey[51], (RMSE = $68 Ha-1; Supplementary Fig. 19).

Figure 3 shows the historic and future ensemble average $Ir_{B/C}$ under a SSP245 emissions trajectory. For completion, we show $Ir_{B/C}$ values for all simulated grid cells. There are many areas throughout the U.S. that irrigate primarily with surface water and estimated pumping costs over these areas may be artificially high. As expected, historically irrigated areas throughout the High Plains have exhibited the highest average annual $Ir_{B/C}$ with a return ratio of approximately 0.76 (Table 1). By mid-century, there is a significant increase in average $Ir_{B/C}$ throughout the north central U.S. and upper Midwest, especially for soybeans. Average $Ir_{B/C}$ over currently irrigated soybean areas in the High Plains increases to 0.59 by mid-century and exceeds maize $Ir_{B/C}$ values by the end of the century (Table 1). Over currently rainfed areas in the midwestern U.S., average annual soybean $Ir_{B/C}$ values become positive by mid-century under a SSP585 future and the end of the century under a SSP245 future. SSP585 end of the century Maize $Ir_{B/C}$ values are negative over most of the U.S. (Table 1 and Supplementary Fig. 20). The difference in average

Table 1 Climate impacts to regional yield and irrigation metrics.

		Corn Belt[a]				High Plains[b]				Eastern Irrigated Area[c]			
		MYG [T Ha-1]	$Ir_{B/C}$[ ]	PRF [%]	WD [mm]	MYG [T Ha-1]	$Ir_{B/C}$[ ]	PRF [%]	WD [mm]	MYG [T Ha-1]	$Ir_{B/C}$[ ]	PRF [%]	WD [mm]
Maize (No adaptation)	Historical	0.83	−0.64	14	−114	4.2	0.76	54	−242	0.89	−0.60	16	−58.1
	Mid SSP245	1.8 (1.3)	−0.22 (−0.45)	31 (23)	−130 (−112)	4.8 (5.0)	1.0(1.1)	60 (65)	−266 (−246)	1.5 (1.4)	−0.33 (−0.39)	26(25)	−69.6 (−55.1)
	Mid SSP585	1.9 (1.3)	−0.17 (−0.46)	33 (22)	−149 (−121)	4.3 (4.6)	0.81 (0.94)	57 (63)	−294 (−256)	1.5 (1.3)	−0.36 (−0.44)	25 (23)	−87.4 (−64.3)
	End SSP245	1.9 (1.1)	−0.17 (−0.53)	33 (18)	−144 (−116)	3.9 (4.2)	0.63 (0.77)	53 (59)	−287 (−263)	1.5 (1.1)	−0.36 (−0.52)	25 (19)	−79.8 (−58.4)
	End SSP585	1.6 (0.82)	−0.33 (−0.65)	27 (10)	−176 (−126)	1.7 (2.2)	−0.32 (−0.075)	25 (34)	−287 (−269)	1.1 (0.79)	−0.53 (−0.64)	17(11)	−111 (−73.5)
Soybean	Historical	0.37	−0.64	14	67.6	1.2	0.15	48	−10.3	0.54	−0.44	24	127
	Mid SSP245	1.0	−0.03	41	44.1	1.7	0.59	62	−43.1	0.99	−0.0067	43	111
	Mid SSP585	1.1	0.10	47	22.0	1.8	0.72	64	−78.7	1.1	0.047	46	79.6
	End SSP245	1.3	0.30	52	25.7	1.8	0.71	67	−75.1	1.2	0.21	51	95.3
	End SSP585	1.6	0.53	64	−34.8	1.7	0.56	62	−161	1.3	0.26	52	31.0

Average irrigated marginal yield gain (MYG), irrigation benefit to cost ratio ($Ir_{B/C}$), irrigation positive return frequency (PRF), and median water deficit (WD), over historically cropped areas in the Corn Belt and irrigated areas in the High Plains and Eastern U.S.
[a]Rainfed areas in: Minnesota, Wisconsin, Michigan, Ohio, Illinois, Indiana, Iowa
[b]Irrigated areas in: Texas, Oklahoma, Kansas, Nebraska
[c]Irrigated areas outside of High Plains, excluding California, Idaho, and Washington

$Ir_{B/C}$ values between longer season and historically grown maize cultivars is most apparent throughout western Minnesota and the Dakotas (Supplementary Fig. 21).

The results above describe only 30-year average irrigation returns. However, farmers often install irrigation equipment as a means of risk mitigation to protect against droughts and within-season climate variability. $Ir_{B/C}$ during the driest year exceeds ~1.5 for nearly all currently irrigated cropland (Supplementary Fig. 22) in the U.S., and we find a significant increase in the frequency in which $Ir_{B/C}$ is positive (Supplementary Figs. 23, 24) during future simulations. The positive return frequency for maize (soybean) in the Corn Belt increases from 14% (14%) to 31% (41%) by mid-century under SSP245 (Table 1) and is relatively consistent across individual members of the 5-member ensemble (Fig. 4)

Although there is variability in growing season precipitation projections between GCMs (Supplementary Figs. 3 and 4), the spatial patterns of average $Ir_{B/C}$ and the frequency in which farmers could expect positive returns from investing in irrigation are relatively consistent across all five GCMs. Figure 4 compares 30-year average maize $Ir_{B/C}$ values and the positive return frequency across the five GCM projections for the mid-century under a SSP245 emissions trajectory. The corresponding mid-century SSP245 soybean GCM correlation matrix is shown in Supplementary Fig. 25. For both maize and soy, the region with the most variability across GCMs appears to be the north central U.S., where average $Ir_{B/C}$ values and positive return frequencies tend to be the lowest under the climate projected from NESM3 GCM and highest under the HadGEM3 GCM. These GCMs correspond with our cool and wet and hot and dry scenarios respectively. During mid-century there is relatively little difference in the spatial patterns of average $Ir_{B/C}$ values and positive return frequencies for a SSP585 emissions trajectory (Supplementary Fig. 26).

Irrigation groundwater deficit. The amount of water available for irrigation is the remaining sum of surface and subsurface flows after accounting for safe environmental flows and other uses. Future estimates of water availability are inherently uncertain as they are heavily dependent on future withdrawals and diversions and explicitly simulating the effects of enhanced or reduced groundwater pumping and surface water diversions is outside the scope of this study. Instead, we approximate the available water for irrigation as the remaining groundwater recharge after accounting for environmental flows and municipal use.

$$\text{Available Water} = (\text{Recharge} - \text{Other Uses}) \quad (1)$$

Recharge rates are simulated directly in rainfed pDSSAT simulations (irrigated simulations don't have a closed water budget) and other uses consist of consumptive uses from industrial and residential sources at the county level[24]. We hold other uses constant in future periods following similar studies[21,52]. Recharge from pDSSAT reasonably approximates existing recharge estimates[53] over the majority of cropped areas in the central U.S. (Supplementary Fig. 27).

Figure 5 shows the average irrigation groundwater deficit (i.e., available water – irrigation water applied) under fully irrigated conditions. While many currently irrigated areas, outlined in black, exhibit near-zero water deficits (or surpluses), there are, unsurprisingly, multiple areas with substantial average annual water deficits. As expected, irrigation in the southern High Plains and California's Central Valley both operate under substantial water deficits during an average growing season. Stippling in Fig. 5 highlights areas with a positive annual $Ir_{B/C}$ values at least once every 3 years. During the historical period, there is little overlap between areas that have a water surplus and areas where irrigation

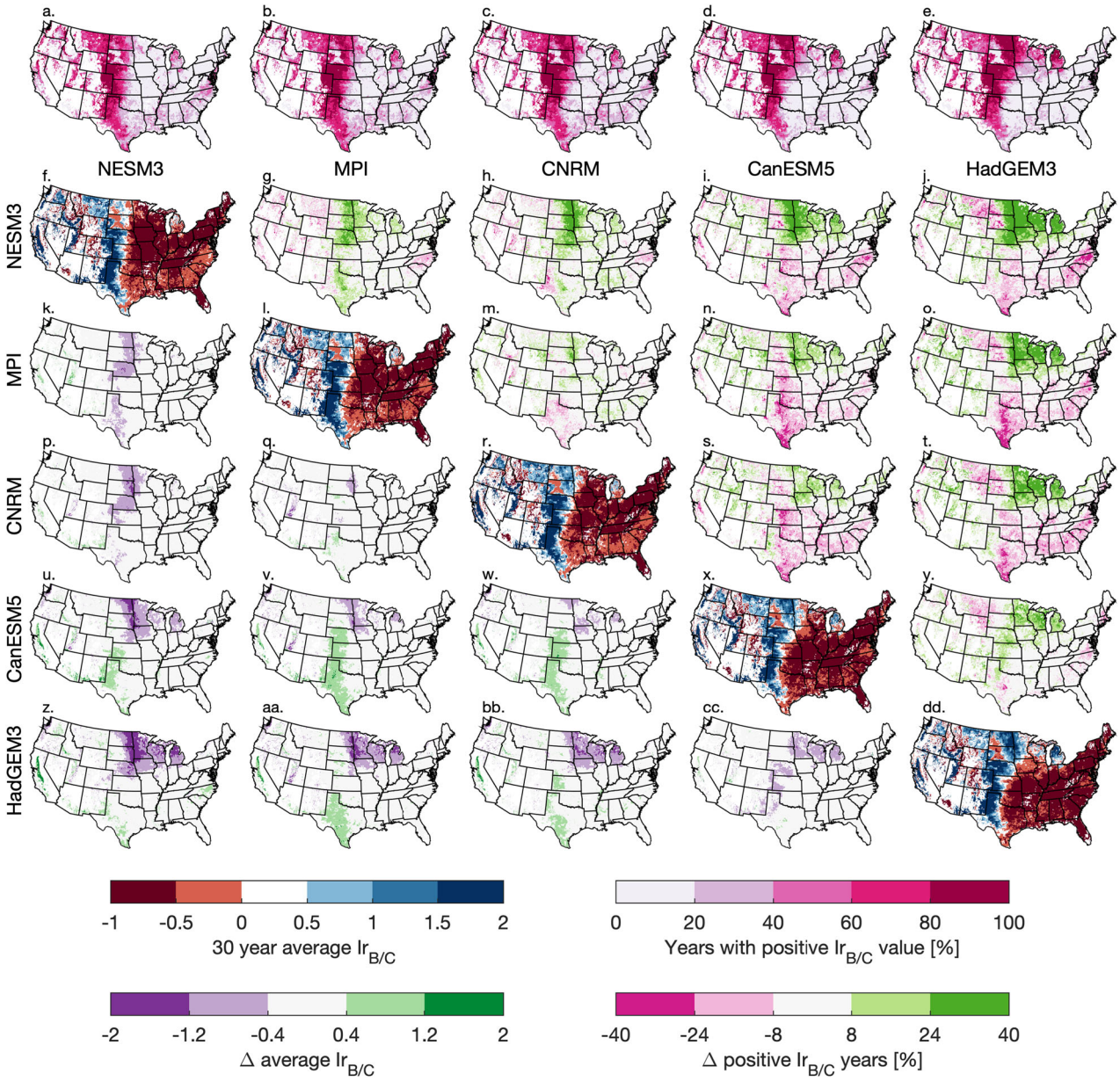

Fig. 4 Inter-model comparison of irrigation benefit to cost ratios and positive return frequencies. SSP245 mid-century (2036–2065) maize $Ir_{B/C}$ positive return frequencies (**a**–**e**) and irrigation benefit to cost ratios (**f**, **l**, **r**, **x**, **dd)** for each GCM in the ensemble. GCM names are provided in column and row headers. Left side of diagonal (**k**, **p**, **q**, **u**, **v**, **w**, **z**, **aa**, **bb**, **cc**) compares $Ir_{B/C}$ between GCMs (rows subtracted from columns) and right side of diagonal (**g**, **h**, **i**, **j**, **m**, **n**, **o**, **s**, **t**, **y**) compares GCM specific $Ir_{B/C}$ positive return frequency (rows subtracted from columns).

returns are routinely positive, with notable exceptions being soybeans grown throughout the Mississippi Valley and parts of the Upper Midwest. In the future, there is an expansion in the area that could expect positive $Ir_{B/C}$ values, but there are also slight decreases in the groundwater deficit throughout most of the country. By mid-century, we find an overlap between areas with positive $Ir_{B/C}$ values and an irrigation water surplus in northern Michigan and Wisconsin for both maize and soybeans and in multiple regions throughout the Corn Belt, Mississippi Valley, and Mid-Atlantic states for soybeans (Fig. 5). Note that our analysis does not explicitly account for the effect of unsustainable groundwater pumping on future groundwater water availability. However, we do find that marginal profits from increased yield could support groundwater pumping from depths that likely exceed most aquifer's saturated thickness through the end of the century under SSP245 (Supplementary Fig. 28).

There is considerable interannual variability in the groundwater deficits. During a wet year, we find a water surplus for almost all presently irrigated soybean regions and most irrigated maize regions outside of the High Plains (Supplementary Fig. 29). Despite the interannual variability in simulated groundwater storage, we find that closing 30-year average annual local water deficits would require up to a 100% reduction in irrigated water applied throughout regions of the southern High Plains (Supplementary Fig. 30).

Discussion

The decision to install irrigation equipment or irrigate during a particular year is multi-faceted. Growers must weigh a number of often competing variables including yearly energy costs, crop market values, seasonal weather forecasts, and previous yield

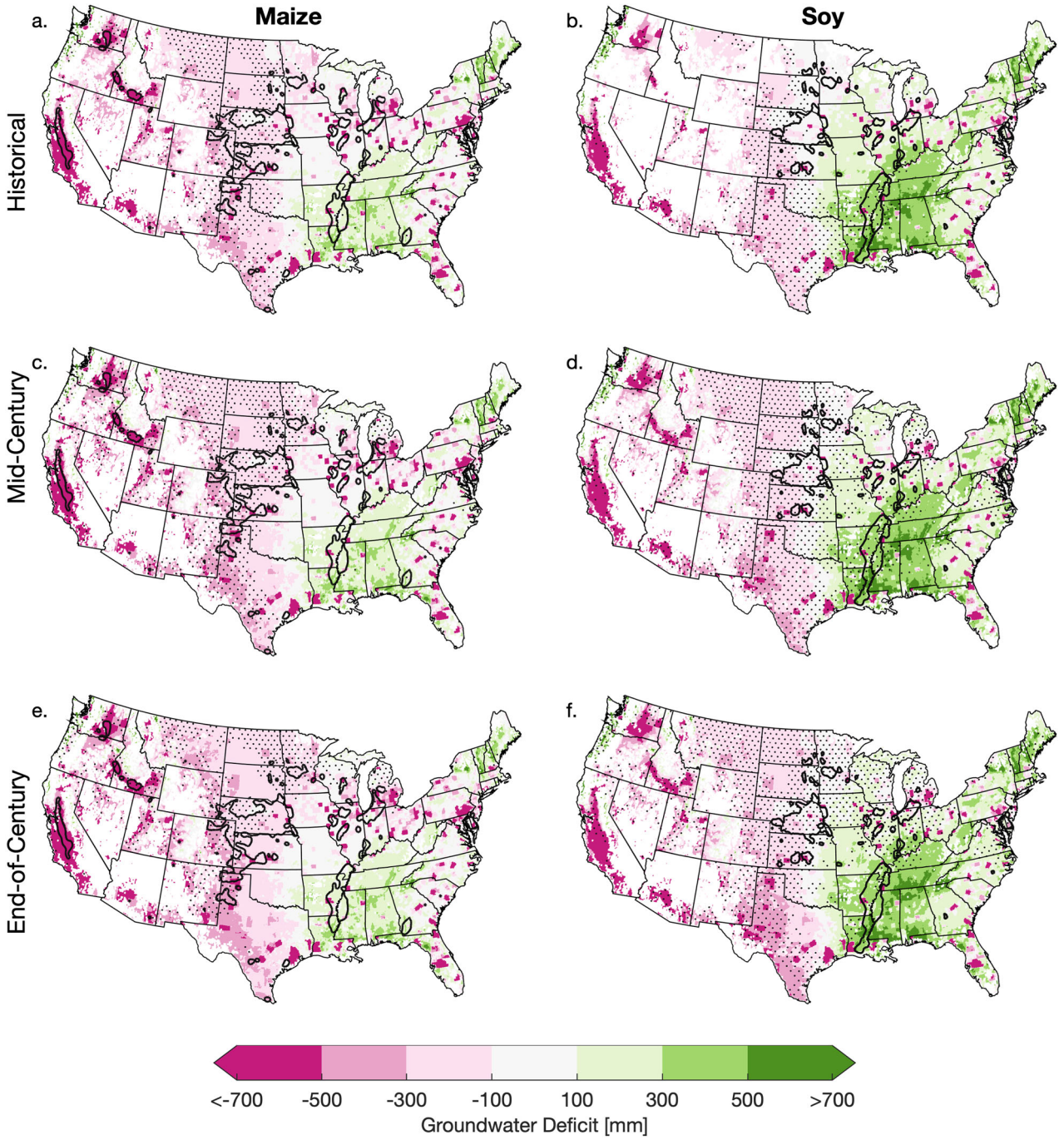

Fig. 5 Average 30-year irrigation groundwater deficit. 30-year average annual irrigation water deficit under fully irrigated conditions under historical (**a**, **b**), mid-century (**c**, **d**), and end-of-century (**e**, **f**) climates for maize (**a**, **c**, **e**) and soybean (**b**, **d**, **j**). Currently irrigated areas for maize and soybean are outlined in black. Irrigation deficit is calculated as the difference between annual groundwater recharge after accounting for other use the total volume of irrigated water applied. Stippling shows grid cells with positive irrigation returns at least once every 3 years.

performance. These decisions are further complicated given the uncertainty of future growing season conditions under climate change and estimates of future irrigation requirements vary considerably between studies. In the Midwest, we find that maize and soybean yields will likely remain near present levels on average with little to no investment in irrigation equipment, at least through mid-century. This underscores recent work[33] as well as early integrated assessments[29,30]. Growing season length is only part of farmers' cultivar selection process[44], but our modeling results suggest that switching to longer season maize cultivars could increase yields by roughly 2 T Ha-1 throughout the Midwest by mid-century relative to historically planted cultivars (Fig. 2 and Supplementary Figs. 14, 15). Soybeans are less sensitive to high temperatures than maize[54] and we find evidence that mid-century rainfed soybean yields could be roughly 1 T Ha-1 higher than present throughout most of the country without shifting cultivars (Fig. 2). Historically irrigated areas throughout the High Plains have realized the greatest return on irrigation investment, but the long-term sustainability of irrigating within the High Plains Aquifer has been a concern for farmers, scientists, and resource managers. Although drilling deeper wells is likely not a successful long-term adaptation strategy[55], we find evidence

that increased pumping costs alone will be insufficient to deter future groundwater use (Supplementary Fig. 28), potentially exacerbating aquifer depletion. The continued positive $Ir_{B/C}$ values throughout the High Plains (Fig. 3) combined with insufficient water resources (Fig. 5) suggest that climate change may incentivize farmers in the High Plains to continue unsustainable irrigation practices, at least throughout the middle of the 21st century. However, unexpected shifts in stakeholder's response to changing conditions can have profound effects on irrigation water use. A stakeholder-driven water conservation initiative in the state of Kansas reduced water use by 31% over a 5 year period[56] and lead to a reduction in overall groundwater withdrawals[57]. Considering these recent successes, future work could critically examine the long-term effects of groundwater conservation initiatives coupled with deficit irrigation under future climates on agricultural productivity and water resource sustainability.

Since the early 2000's, farmers have been installing irrigation on previously rainfed croplands throughout the Midwest and Southeast[58], and recent studies have found that these regions could be suitable for sustainably expanded irrigation with some investment in water holding infrastructure[21]. Our results suggest that groundwater could support irrigated soybean throughout most of the eastern U.S. and irrigated maize in some regions of the Southeast, but we find little to no net economic benefit of irrigating maize or soybean throughout most of the eastern U.S. during an average year (Fig. 3). The frequency of drought is expected to increase in the future[59] and irrigation is often installed as a risk mitigation measure against drought[60,61] which may not be used continuously from one year to the next. We find evidence that expanded irrigation could play an important role in mitigating the impacts of drought throughout most of the U.S. (Supplementary Fig. 22), with substantial increases in the number of years that farmers could expect positive returns from irrigating, especially throughout the Corn Belt and eastern U.S. (Table 1 and Supplementary Figs. 23, 24). It is important to note that there are often institutional incentives for installing irrigation equipment which we did not consider in our cost benefit analysis. The installation of irrigation as a mitigation measure against drought is influenced by policy incentives as well as farmers' individual risk tolerance. As insurance premiums increase with warmer growing season temperatures[62,63], farmers may be further incentivized to install irrigation equipment. This could lead to further groundwater depletion and other water resource challenges in areas without sufficient groundwater recharge rates. Assuming a theoretical desirability threshold of positive $Ir_{B/C}$ values at least once every 3 years we find that groundwater could support the expanded and routinely profitable irrigation of soybean throughout many regions of the Corn Belt, southern Mississippi Valley, Mid-Atlantic, as well as northern Michigan and Wisconsin. The higher water demand and greater temperature sensitivity of maize limits areas where groundwater could support expanded sustainable and profitable irrigation to northern Michigan and Wisconsin (Fig. 5). While a high emissions future is increasingly unlikely, end-of-century SSP585 maize production could be severely limited across many historically productive regions (Supplementary Fig. 12). The increased productivity and lower irrigation water requirements of soybean could have cascading implications for crop rotations, markets, and consumers. Future work could explore the economic, social, and environmental tradeoffs associated with expanding soybean production over areas that have historically produced maize.

Economic pressure for irrigation expansion in Montana, North Dakota, and South Dakota may create future water resource challenges. These areas all experience high $Ir_{B/C}$ ratios for both maize and soy by mid-century (Fig. 3) but do not have additional groundwater resources available to support widespread sustainable expansion (Fig. 5). These three states are underlain by a combination of thick sandstone aquifers and glacial sediments that could provide abundant water resources for short- to medium-term production[64]. However, like the High Plains Aquifer to the south, expanded irrigation in much of the region would not be sustainable. Policy makers can respond to these projections by putting in place measures that account for local resource sustainability in allowing large-scale groundwater withdrawals.

Irrigation water use decisions are highly variable across time and space and may not necessarily be explained by differences in crop choice, weather, infrastructure, or soil[65]. Here, we have made several simplifying assumptions to approximate irrigation costs and benefits at the continental U.S. (CONUS) scale. For example, irrigation pump and application efficiencies will vary considerably with the type and age of irrigation system and ownership costs depend on the size and type of system being installed as well as local socioeconomic variables such as labor rates, interest rates, insurance premiums, and external incentives. The average irrigation ownership cost for a central pivot system ($337 hectare-1) was acquired from four available extension documents with estimates that range from $189 to $405 hectare-1 (Supplementary Table 2). Ownership costs account from ~20% to nearly 100% of total operational costs depending on the depth to groundwater, and consequently pumping costs. As such $Ir_{B/C}$ values are sensitive to the approximated ownership costs, but the overall patterns shown in Fig. 3 are relatively consistent for ownership costs of $189 and $405 (Supplementary Fig. 31).

There are several important limitations to our modeling framework and analysis that should be noted. Here we discuss five primary limitations of this work and provide suggestions for addressing these limitations in future work. First, we do not account for changes in depth to groundwater due to shifting withdrawal rates. Simulated recharge rates within pDSSAT do account for changes to precipitation and evapotranspiration, but those changes are small relative to the potential impact of increasing (or decreasing) withdrawals. As such, our results reflect the isolated climatological impact on maize and soybean irrigation profitability and sustainability under present groundwater availability. A theoretical 20% increase in the depth to groundwater has minimal impact on the spatial pattern of $Ir_{B/C}$ values (Supplementary Fig. 32). Developing future CONUS scale groundwater availability scenarios with evolving land use and withdrawal rates would be a substantial contribution to evaluating future water availability. Further, our results could influence existing land use projections such as those from the Land Use Harmonization project[66]. A comparison of land use projections with water availability and agricultural productivity could inform land use optimization for agriculture, renewable energy development, residential use, and other development. Second, we utilized a simplified irrigation scheme within pDSSAT and our $Ir_{B/C}$ analysis. Crops in pDSSAT are irrigated with 10 mm of water anytime plant available water falls below 40% throughout the growing season. Many regions have successfully promoted deficit irrigation (a practice of applying less water than is required to meet the full crop evapotranspiration demand) as it has demonstrated to have minimal impact on yields while conserving water use[67]. Simulating future crop productivity under various deficit irrigation strategies could help identify regions, crops, and management strategies that optimize tradeoffs between productivity and water use. Third, future adaptations to crop selection and other management decisions are difficult to predict. As already mentioned, climate is only one component of a complex decision making process that farmers undertake when selecting cultivars and planning for the future[44]. We have approximated maize cultivar

shifts as a function of climate and evaluated the consequences of those shifts against maintaining historic maize cultivars, but there will likely be unforeseen shifts in cropping practices that will invalidate our assumptions. Fourth, our modeling exercise does not account for the influence of irrigation on local and regional climate, which has been shown to be important throughout regions of the U.S.[68,69]. While irrigation induced changes to local and regional climate are likely secondary to climate change effects, future work exploring the land-atmosphere feedbacks between future changes in irrigated agriculture (and other agricultural management practices) could help constrain regional climate projections. Fifth and finally, our results may be dependent on inherent biases and limitations within pDSSAT. As the focus of this work is to explore the potential feasibility of current and expanded irrigation across a range of future climate projections, we opted to use a single crop model driven with an ensemble of climate projections. While we can't directly evaluate pDSSAT against other crop models, recent crop model intercomparison projects have reported that pDSSAT tends to have the highest skill at simulating maize growth in the U.S.[70].

Conclusion

Irrigation is an essential component of U.S. agriculture. Climate change will alter both crop water demands and the amount of water available for irrigation. Using a 5-member ensemble of future climate scenarios across multiple emissions trajectories we find significant changes in marginal yield gains from irrigating and corresponding irrigation benefit-to-cost ($Ir_{B/C}$) values. By mid-century, there are significant increases in marginal yields throughout the north central U.S. and upper Midwest for maize, and most of the central U.S. for soybean. Higher marginal yield values lead to an increase in the average $Ir_{B/C}$ values throughout the Dakotas, Northern Michigan, Wisconsin, and eastern Texas. This could potentially incentivize farmers in the region to install irrigation and place additional pressures on groundwater resources. In the Corn Belt, we find little to no increase in maize and soybean marginal yields. Average annual rainfed maize and soybean yields could continue to increase throughout the majority of the Corn Belt, at least throughout the mid 21st century. Warmer temperatures and shifting precipitation patterns will likely result in more frequent drought conditions throughout the Corn Belt and having the ability to irrigate during a dry year will be increasingly advantageous. However, our results suggest that the costs of irrigating will outweigh the benefits over the long term unless there are external incentives to reduce ownership and operational costs.

The feasibility of future sustainable irrigation hinges on the availability of water suitable for agricultural use. As agriculture is the single largest consumer of water in the country and future water resources are uncertain, it is critical to weigh the tradeoffs from allocating additional water resources to agricultural use. Expanded soybean irrigation may be feasible and profitable throughout multiple regions of the eastern U.S. and could be an important component to help adapt agricultural systems to climate change. Some regions in the northern Midwest could expect increased yields and routinely positive returns from irrigating maize, potentially incentivizing agricultural intensification in this area. It will be important for decision makers throughout the U.S. to understand and account for local water demand and availability when developing policies guiding irrigation installation and use.

Data and methods

Experimental design. This main objective of this study was to explore the economic feasibility of both current and expanded irrigation for maize and soybean across the contiguous United States (CONUS) for a range of projected climate futures. To address this question, we developed a research framework consisting of four main components: (I) crop model calibration and evaluation, (II) GCM selection and downscaling, (III) running historic and future crop simulations, and (IV) post-processing crop model output to derive feasibility indices. Each component is briefly described in the following paragraphs with additional detail in the following subsections.

We ran pDSSAT for three 30-year periods: a historical period from 1981–2010, a mid-century period from 2036–2065, and an end-of-century period from 2071–2100. To explore the uncertainty in future climate projections we used a five-member ensemble of statistically downscaled GCMs from the sixth phase of the Climate Model Intercomparison Project (CMIP6) under both medium and high future emissions trajectories or Shared Socioeconomic Pathways - SSP245 and SSP585 respectively. SSP585 (SSP245) represents a high emissions (middle of the road) future and is comparable to the RCP8.5 (RCP4.5) emission trajectory from CMIP5[71]. Details of the GCM selection process and downscaling approach are described below.

Historic simulations were calibrated using county level data on crop management and progress data such as planting date, maturity date, and harvest date, and evaluated against county level yield data. Future crop simulations attempt to account for potential adaptations to planting date and cultivar selection through modifying management and crop physiological parameters.

We assess the feasibility of current and future irrigation through two main indices, the irrigation benefit to cost ratio ($Ir_{B/C}$) and the irrigation water deficit. Each index is calculated for maize and soybean over all currently cultivated land in the CONUS. Briefly, irrigation benefits are approximated as the marginal yield gained from irrigating, and irrigation costs are calculated based on an estimate of pumping and ownership costs. Irrigation water deficit is the difference between approximated water available for irrigation (after accounting for other uses) and simulated irrigation requirements.

Crop model input and calibration data. We simulated daily maize and soybean growth on a 5-arcminute grid over all historically cultivated areas in the CONUS for historical and future periods. Both maize and soybean were simulated using version 4.6 of the Decision Support for Agrotechnology Transfer[38,72] modeling ecosystem using the CERES-Maize[73] and CROPGRO-Soybean[74,75] models respectively. DSSAT is a point-based biophysical modeling framework that links multiple cropping system models to simulate crop growth as a function of weather, soil, management, and nutrient availability. We parallelize DSSAT to operate on the aforementioned 5 arcminute grid using the parallelized System for Integrating Impacts Models and Sectors (pSIMS)[37], and herein refer to the gridded model as pDSSAT. At a minimum, pDSSAT requires the following input data: (I) daily values of maximum and minimum temperature, precipitation, and solar radiation, (II) detailed soil profile data such as soil horizon depths, percentage sand, silt, and clay, bulk density, organic carbon content, pH, and root abundance; (III) management data such as planting date, planting density, planting depth, row spacing, fertilizer practices, irrigation rates, and detailed crop growth parameters. We utilize daily meteorological data from the Livneh dataset, which assimilated data from roughly 20,000 weather stations into the Variable Infiltration Capacity Hydrologic model to provide daily gridded hydrometeorological data at a 1/16° horizontal resolution for the CONUS, Mexico and southern Canada[76,77]. The datasets used here to calibrate, evaluate, and force pDSSAT are listed in Table 2 and a detailed description of the calibration approach is included below. For each 30-year time period, pDSSAT was run in sequence with a

Table 2 Data sources for forcing and calibrating pDSSAT simulations, and calculating the $Ir_{B/C}$ and irrigation water deficit values.

Data Type	Data	Source
pDSSAT input and forcing	Daily meteorological forcing data	Livneh et al.[76]
	Future climate projections	CNRM-CM6: Voldoire (2019)
		CanESM5: Swart et. al., (2019)
		HadGEM3-GC31-LL: Good (2019)
		MPI-ESM1-2-LR: Wieners et. al., (2019)
		NESM3: Cao, Jian (2019)
	Gridded soil textures	Shangguan et al., (2014)
	Global atmospheric CO2	Meinshausen et al. (2020)
	Fertilization rates	Lopez et al.[20]
	U.S. cultivated area	Boryan et al.[81]
pDSSAT calibration and evaluation	Irrigated Area	Pervez & Brown[82]
	County crop yield	USDA NASS Quickstats
	County crop progress dates	USDA NASS Quickstats
	State planting density	USDA NASS Quickstats
	Irrigation application rates and pumping costs	2013 USDA Farm and Ranch Irrigation Survey
	Groundwater recharge rates	Reitz et. al.[53]
$Ir_{B/C}$ and water deficit calculation	Depth to groundwater and transmissivity	Zell & Sanford[49]
	Energy costs	U.S. Energy Information Association
	Irrigation ownership and maintenance costs	See Table S2
	Irrigation application and pump efficiency	McCarthy et al.[48]; New (1988)
	Industrial and municipal water use	Dieter et al.[24]

fallow period between harvest and planting to prevent the re-initialization of soil conditions at the beginning of each growing season, which introduces significant biases[78].

We used the CERES-Maize module within pDSSAT to simulate maize growth. CERES-Maize estimates plant growth through accumulated thermal energy, approximated as Growing Degree Days (GDDs) above an 8 °C threshold. Cultivar differences are accounted for through six crop parameters: *p1* approximates the accumulated GDDs from plant emergence to the end of the juvenile period; *p2* is the development delay for each daylight hour above 12.5 h; *p5* is the GDDs required for plants to progress from silking to maturity; *g2* is the maximum kernel number per plant; *g3* is the kernel growth rate during optimum conditions; *PHIT* is the thermal time between successive leaf tips. Here, we approximated historical values of *p1* and *p5* using weekly crop progress data from the USDA NASS, and the remaining maize parameters follow Lopez et al.[20] Specifically, we calculated the total accumulated GDDs during the interval from plant emergence to tassel initiation and silking to physiological maturity based on when 50% of plants in each state have surpassed the respective threshold (i.e., sowing, emergence, silking, maturity). Since observations of tassel initiation do not exist in the NASS dataset, we approximated *p1* using the relationship between tassel emergence, estimated here as 14 days prior to silking, and tassel initiation:[79]

$$\mathrm{GDD_{TI}} = 0.46 * \mathrm{GDD_{TE}} - 25.9 \quad (2)$$

Where GDD_{TI} is the accumulated GDDs between plant emergence and tassel initiation and GDD_{TE} is the accumulated GDDs between plant emergence and tassel emergence.

We simulated soybean growth using the CROPGRO-Soybean module within pDSSAT[74,80]. Soybean development is a function of both temperature and photoperiod. Within CROPGRO, soybean response to photothermal time varies with plant growth stage and cultivar. pDSSAT contains 13 soybean Maturity Groups (MGs) with 8 varietals in each group. Cultivars are organized from cooler/longer day varietals, typically planted in higher latitudes, to warmer/shorter day varietals, typically planted in lower latitudes. Growers in the U.S. typically plant soybean varietals ranging from MG 00 in the northern plains to MG 09 in southern Florida[43]. To approximate historical soybean varietals, we calculated accumulated photothermal time between average historical plant emergence and plant maturity dates from NASS and linearly mapped the range of values to soybean cultivar indices.

After estimating maize and soybean phenological parameters, we calibrated simulated yield to observed county yield from NASS by modifying the planting density as well as the maximum kernel number *(g3)* for maize and the cultivar ID for soybean. State level planting densities were acquired from USDA NASS[23]. We linearly increased the kernel number from 730 in 1980 to 790 in 2010[20] and soybean cultivar ID numbers were approximated annually based on temperature and photoperiod as described above. Finally, we iteratively adjusting the Soil Level Productivity Factor (SLPF) in pDSSAT. We ran irrigated and rainfed simulations with SLPF values varying from 0.05 to 1.0 from 1991–2000 and assigned county-level SLPF values that minimized the RMSE between county-level observed and simulated yields. To aggregate simulated yields from the 5-arcminute resolution to the county level we used a crop-specific irrigated area map developed by ref. [20] Maps of crop specific irrigated and rainfed area are shown in Supplementary Fig. 11. The irrigation map was calculated by combining crop distribution data from the USDA NASS Cropland Data Layer[81] with county level irrigated area statistics from the Moderate Resolution Imaging Spectroradiometer Irrigated Agriculture Dataset for the United States (MIrAD)[82]. After estimating county level SLPF values, we evaluated simulated yields against reported county-level yields from 2001–2010.

Future advancement in plant breeding could lead to increased yield potential for maize and soybean while also increasing their resilience to environmental stress. As projecting these advancements adds additional uncertainty to our analysis, we hold crop physiological parameters static for future periods and allow for relatively simple adaptations in planting date and cultivar selection. Shifting planting dates is one of the easiest adaptations that growers can make. We approximated future planting dates for maize and soybean using a random forest algorithm trained on historical planting dates and 6 predictor variables: (1) February – April accumulated Growing Degree Days (GDDs); (2) February – April average daily Standardized Precipitation-Evapotranspiration Index (SPEI); (3) February – April average

temperature; (4) February – April total precipitation; (5) average state latitude, (6) average state longitude. The trained random forest reasonably recreates statewide historical maize planting dates (out of the box r^2 of 0.88), but struggles to capture historic soybean planting dates (out of the box $r^2 = 0.21$).

We simulated future maize growth using both historic and shifted cultivars. Future shifts in maize cultivars were approximated by scaling historic estimates of *p1* and *p5* by the change in accumulated GDDs during their respective periods under historical and future climate for each time period, GCM, and SSP scenario, yielding a climate specific cultivar map. Other maize parameters (*g2, g3, and* PHINT*)* are kept static in future simulations. We held soybean varietals constant for all future simulations given the relatively large temperature bands of soybean maturity groups[43].

GCM selection and downscaling. pDSSAT was forced with climate projections from 5 GCMs from the CMIP6 archive and statistically downscaled to 1/16° horizontal resolution. We selected 5 GCMs that cover the projected range in future temperature and precipitation for the Midwest based through comparing projected changes in average annual temperature (ΔT) and precipitation (ΔP) for the Midwest from 2071–2100 under SSP585 (Supplementary Fig. 2)[83]. We next identified the 10th, 50th, and 90th percentile values of ΔT and ΔP. These values represent the median as well as the four corners of the range of possible futures (e.g., hot and dry, cool and wet, etc.). Second, we calculated the proximity of each model simulation to the 10th, and/or 90th, and 50th percentiles of ΔT and ΔP using the model's *z*-scores to weight changes in temperature and precipitation evenly.

$$D_{z_i^T, z_i^P} = \sqrt{\left(\left(|z_i^T - z_i^T|\right)^2 + \left(|z_i^P - z_i^P|\right)^2\right)} \quad (3)$$

Where $D_{z_i^T, z_i^P}$ is the distance of a model (j)'s ΔT and ΔP to either the corner or middle (i)'s 10th, 50th, and/or 90th percentile. We then selected the 5 models with the lowest value of *D* for each corner and the inter-model median. Finally, of the 5 selected models at each intersection, we selected the single model that best recreates historical climate (Supplementary Fig. 1) based on a combined skill score (S_{hist}) which averages independent skill scores of temperature (S_T) and precipitation (S_P). S_T measures the overlapping area between probability density functions of simulated and observed monthly temperature values.

$$S_T = \sum_i^n \min(Z_{GCM}, Z_{Obs}) \quad (4)$$

Where n is the number of bins in the pdf, Z_{GCM} is the frequency of simulated values in a given bin, and Z_{Obs} is the frequency of observed values in a given bin. If a model simulates observed temperature perfectly, S_T will be equal to 1. S_P consists of six functions that each consider a different aspect of precipitation[84].

$$S_{P1} = 1 - \left(\frac{|A_{GCM} - A_{Obs}|}{2 * A_{Obs}}\right)^{0.5} \quad (5)$$

$$S_{P2} = 1 - \left(\frac{|A^+_{GCM} - A^+_{Obs}|}{2 * A^+_{Obs}}\right)^{0.5} \quad (6)$$

$$S_{P3} = 1 - \left(\frac{|A^-_{GCM} - A^-_{Obs}|}{2 * A^+_{Obs}}\right)^{0.5} \quad (7)$$

$$S_{P4} = 1 - \left(\frac{|\underline{P_{GCM}} - \underline{P_{Obs}}|}{2 * \underline{P_{Obs}}}\right)^{0.5} \quad (8)$$

$$S_{P5} = 1 - \left(\frac{|\sigma_{GCM} - \sigma_{Obs}|}{2 * \sigma_{Obs}}\right)^{0.5} \quad (9)$$

$$S_{P6} = 1 - (\mathrm{nRMSE}_{GCM})^{0.5} \quad (10)$$

A_{GCM} and A_{Obs} are the areas below the cumulative distribution functions of simulated and observed precipitation and $A+$ and $A-$ are the areas right and left of the 50th percentile. Functions S_{P1} through S_{P3} represent the ability of the model to simulate the entire precipitation distribution, high precipitation events, and low precipitation events, respectively. *P* is the mean total precipitation over the Midwestern U.S. and σ is the standard deviation of the precipitation pdf. Thus, a model's ability to recreate historical average precipitation and precipitation variability is accounted for through S_{P4} and S_{P5} respectively. S_{P6} was added here to measure a model's ability to recreate the monthly seasonal cycle of precipitation, where nRMSE is the normalized root mean square error between simulated and observed monthly seasonal precipitation cycles. The six scores are simply multiplied to create a single score for precipitation (S_P), where 1 would represent perfect agreement between simulated and observed precipitation. The overall model skill (S_{hist}) is calculated as the average between S_T and S_P.

$$S_{hist} = \frac{S_T + S_P}{2} \quad (11)$$

The final 5 GCMs, which represent a range of possible futures, from relatively cool and dry to hot and wet, are shown in Supplementary Table 1. Although the models were selected based on the SSP585 scenario from 2071–2100, for simplicity we use the same models for all future time periods.

Future climate projections were statistically downscaled using a delta change approach. Monthly GCM outputs were used to create seasonal cycles for historical (1981–2010) and future (2036–2065 & 2071–2100) periods for both SSP245 and SSP585 for each of the final 5 GCMs. Monthly differences between a GCM's historical and future simulations were interpolated to the Livneh grid and applied to daily observations (additive for temperature and multiplicative for precipitation and solar radiation). While relatively simple to implement, the delta change approach reduces future bias in GCM simulations, while retaining historical climate variability and is commonly used in climate impact studies.

Irrigation value. We calculated the irrigation benefit to cost ratio ($Ir_{B/C}$) for each grid cell (i,j*)* and growing season (y*)* relative to the associated operational costs:

$$Ir_{B/C} = \frac{\Delta Y_{c,i,j,y} * MP_c}{P_{c,i,j,y} + O_y} - 1 \quad (12)$$

Where $\Delta Y_{c,i,j,y}$ is the grid cell specific marginal yield gain for a given crop (c*)*, MP_c is the market price for that crop, here MP_c is defined as the 2000–2020 average international market price for maize and soybean from the FAO's Food Price Monitoring and Analysis Tool ($160 and $365, respectively)[85] and held constant for future time periods. $P_{c,i,j,y}$ are the pumping costs of irrigating crop c in grid cell i,j during growing season y and O_y are annual ownership costs. While ownership costs will vary considerably based on specific application, we assume a central pivot system covering a quarter-mile field with a 20-year life cycle and calculate an average ownership cost from multiple extension documents (Supplementary Table 2). Pumping costs are calculated through combing regional energy costs from the US Energy

Information Administration (Supplementary Fig. 18)[47] with the total energy required for pumping (E_D)[48]. Specifically:

$$E_D = \rho g V L_T \times \varepsilon_P \quad (13)$$

Where ρ is the density of water, g is gravitational acceleration, V is the volume of water being pumped over the growing season, ε_P is the pumping efficiency which we assume to be 0.77[86], and L_T is the total lift required for pumping, calculated as:

$$L_T = L_{WT} + L_{CD} + L_{WD} + L_{PR} \quad (14)$$

Where L_{WT} is the depth to water table[49] interpolated to the pDSSAT grid, L_{CD} is the additional lift required due to the cone of depression that forms around the well during pumping, L_{WD} is the additional lift due to drawdown within the well, and L_{PR} is the effective lift due to pipe pressurization. We calculate the combined lift required from the cone of depression (L_{CD}) and pipe drawdown (L_{WD}) using the following equation:

$$L_{CD+WD} = 1.5 \times \frac{Q}{4\pi T}\left[-0.5772 - \ln\left(\frac{r^2 S}{4Tt}\right)\right] \quad (15)$$

Where Q is the pumping rate, T is the spatial varying transmissivity[49] and S is the specific yield approximated here as 0.2. We assume a uniform well radius (r) of 9 inches and a static irrigation period (t) of 90 days. Accounting for 50% well drag, we multiply L_{CD+WD} by 1.5. An example of pumping depth components is shown in Supplementary Fig. 33.

Water deficit. We calculate the water deficit as the difference between total water applied within a simulation and the amount of water that could sustainably be available for irrigation. Groundwater available for irrigating is calculated using simulated surficial runoff and subsurface drainage from pDSSAT. Specifically:

$$\text{Available Water} = (\text{Recharge} - \text{Other Uses}) \quad (16)$$

Where recharge is simulated directedly within pDDSAT as subsurface drainage, providing a consistent scenario-specific approximation of recharge throughout CONUS. Other uses consist of consumptive uses from industrial and residential sources at the county level[24], which are held constant in future periods.

Data availability

The DSSAT model output data and campaign files used to generate the results of this paper are publicly available at https://doi.org/10.5281/zenodo.7747561. DSSAT input data used here are listed in Table 2. The Livneh meteorological dataset can be downloaded from the NOAA Physical Science Laboratory (https://psl.noaa.gov/data/gridded/data.livneh.html). CMIP6 data are archived at the Lawrence Livermore National Laboratory (https://esgf-node.llnl.gov/projects/cmip6/). The Global Soil Dataset for use in Earth System Models can be found at https://doi.org/10.1002/2013MS000293. Model parameterization data such as crop progress dates, crop yields, planting densities, and cultivated area can be acquired from the U.S. Department of Agriculture National Agricultural Statistic Service (https://www.nass.usda.gov/Quick_Stats/). Regional energy prices used in the calculation of groundwater pumping costs are listed by the U.S. Energy Information Association (https://www.eia.gov/electricity/state/).

Code availability

The DSSAT crop model can be downloaded from the DSSAT webpage (https://dssat.net/). The parallel System for Integrating Models and Sectors (pSIMS) is open source and is available on the RDCEP github (https://github.com/RDCEP/psims). Scripts used for downscaling CMIP6 data, creating model campaign files, and analyzing model output is available from the corresponding author upon request.

Received: 28 October 2022; Accepted: 12 June 2023;
Published online: 14 August 2023

References

1. Hayhoe, K. et al. Our Changing Climate. in *Impacts, Risks, and Adpataion in the United States* 72–144 (U.S. Global Change Research Program, 2018).
2. Tilman, D., Balzer, C., Hill, J. & Befort, B. L. *Proc. National Academy of Sciences of the United States of America* **108** 20260–20264 (2011).
3. Valin, H. et al. in *Agricultural Economics* Vol. 45, 51–67 (John Wiley & Sons, Ltd, 2014).
4. van Dijk, M., Morley, T., Rau, M. L. & Saghai, Y. in *A Meta-Analysis of Projected Global Food Demand and Population at Risk of Hunger for the Period 2010–2050, Nature Food* Vol. 2 494–501 (Nature Publishing Group, 2021).
5. Lobell, D. B., Schlenker, W. & Costa-Roberts, J. Climate trends and global crop production since 1980. *Science* **333**, 616–620 (2011).
6. Ortiz-Bobea, A., Ault, T. R., Carrillo, C. M., Chambers, R. G. & Lobell, D. B. in Anthropogenic climate change has slowed global agricultural productivity growth. *Nature Climate Change 2021* Vol. 11, 306–312 (Nature Publishing Group, 2021).
7. Lesk, C. et al. in *Nature Reviews Earth & Environment* Vol. 3 872–889 (Nature Publishing Group, 2022).
8. Rosa, L. in *Environmental Research Letters* Vol. 17, 063008 (IOP Publishing, 2022).
9. Ward, F. A. in *Journal of Environmental Management* Vol. 302, 114032 (Academic Press, 2022).
10. Jägermeyr, J. et al. in *Environmental Research Letters* Vol.11, 025002 (IOP Publishing, 2016).
11. Mueller, N. D. et al. in *Nature 2012 490:7419* Vol. 490, 254–257 (Nature Publishing Group, 2012).
12. Rosa, L. et al. in *Environmental Research Letters* Vol. 13, 104002 (IOP Publishing, 2018).
13. Jägermeyr, J., Pastor, A., Biemans, H. & Gerten, D. in Reconciling irrigated food production with environmental flows for Sustainable Development Goals implementation, *Nature Communications* Vol. 8, 1–9 (Nature Publishing Group, 2017).
14. Zipper, S. C. et al. in Quantifying Streamflow Depletion from Groundwater Pumping: A Practical Review of Past and Emerging Approaches for Water Management, *JAWRA Journal of the American Water Resources Association* Vol. 58, 289–312 (John Wiley & Sons, Ltd, 2022).
15. Scanlon, B. R. et al. in Groundwater depletion and sustainability of irrigation in the US High Plains and Central Valley. *Proc. National Academy of Sciences of the United States of America* Vol. 109, 9320–9325 (2012).
16. Sapkota, A., Haghverdi, A., Avila, C. C. E. & Ying, S. C. Irrigation and greenhouse gas emissions: a review of field-based studies. *Soil Systems* Vol. 4, 20 (Multidisciplinary Digital Publishing Institute, 2020).
17. Cotterman, K. A., Kendall, A. D., Basso, B. & Hyndman, D. W. in *Climate Change* Vol. 146, 187–200 (Springer Netherlands, 2018).
18. Döll, P. & Siebert, S. in *Water Resources Research* Vol. 38 (American Geophysical Union (AGU), 2002).
19. Elliott, J. et al. in *Proc. National Academy of Sciences of the United States of America* **111** 3239-3244 (National Academy of Sciences, 2014).
20. Lopez, J. R. et al. in *Earth's Future* **10** e2021EF002018 (John Wiley & Sons, Ltd, 2022).
21. Rosa, L. et al. in *Proceedings of the National Academy of Sciences of the United States of America* Vol. 117, 29526–29534 (National Academy of Sciences, 2020).
22. Tigchelaar, M., Battisti, D. S., Naylor, R. L. & Ray, D. K. in *Proc. National Academy of Sciences of the United States of America* Vol. 115, 6644–6649 (National Academy of Sciences, 2018).
23. USDA NASS 2018 USDA—National Agricultural Statistics Service—Quick Stats [Data file] (https://nass.usda.gov/Quick_Stats/) (Retrieved: 01 March 2021).
24. Dieter, C. A. et al. Five-year clinical outcome and valve durability after transcatheter aortic valve replacement in high-risk patients: FRANCE-2 Registry. *Circular* **138**, 2597–2607 (2018).
25. Rosenberg, N. J., Brown, R. A., Izaurralde, R. C. & Thomson, A. M. in *Agricultural and Forest Meteorology* Vol. 117, 73–96 (Elsevier, 2003).
26. Thomson, A. M., Rosenberg, N. J., Izaurralde, R. C. & Brown, R. A. in *Climatic Change* Vol. 69, 89–105 (Springer, 2005).
27. Li, X. & Troy, T. J. in *Environmental Research Letters* Vol. 13, 064031 (IOP Publishing, 2018).
28. Wang, X. et al. in *Nature Communications* Vol. 12, 1-8 (Nature Publishing Group, 2021).
29. Reilly, J. et al. in U.S. agriculture and climate change: new results. *Clim. Change* **57** 43–67 (2003).
30. Strzepek, K. M. et al. in *Journal of the American Water Resources Association* Vol. 35, 1639–1655 (American Water Resources Assoc, 1999).
31. Lobell, D. B. et al. in *Science* Vol. 344, 516–519 (American Association for the Advancement of Science, 2014).

32. Ort, D. R. & Long, S. P. in *Science* Vol. 344, 484–485 (American Association for the Advancement of Science, 2014).
33. Basso, B., Martinez-Feria, R. A., Rill, L. & Ritchie, J. T. in Contrasting long-term temperature trends reveal minor changes in projected potential evapotranspiration in the US Midwest. *Nat. Commun.* **12**, 1–10 (Nature Publishing Group, 2021).
34. Partridge, T. F. et al. in *Environmental Research Letters* Vol. 14 (IOP Publishing, 2019).
35. Lopez, J. R. et al. Integrating growth stage deficit irrigation into a process based crop model. *Agric. For. Meteorol.* **243** 84–92 (2017).
36. D'Odorico, P. et al. in *Proc. National Academy of Sciences of the United States of America* Vol. 117, 21985–21993 (National Academy of Sciences, 2020).
37. Elliott, J. et al. in *Environmental Modelling & Software* Vol. 62, 509–516 (Elsevier, 2014).
38. Jones, J. W. et al. in *European Journal of Agronomy* Vol. 18, 235–265 (Elsevier, 2003).
39. Qian, B. et al. in *Scientific Reports* Vol. 11, 1–12 (Nature Publishing Group, 2021).
40. Riahi, K. et al. in *Global Environmental Change* Vol. 42, 153–168 (Pergamon, 2017).
41. Cao, J. et al. in *Geoscientific Model Development* Vol. 11, 2975–2993 (Copernicus GmbH, 2018).
42. Christidis, N. et al. A New HadGEM3-A-Based System for Attribution of Weather- and Climate-Related Extreme Events. *J. Climate* **26**, 2756–2783 (2013).
43. Mourtzinis, S. & Conley, S. P. in *Agronomy Journal* Vol. 109, 1397–1403 (American Society of Agronomy, 2017).
44. Abendroth, L. J. et al. in *Global Change Biology* Vol. 27, 2426–2440 (John Wiley & Sons, Ltd, 2021).
45. Kunkel, K. E., Easterling, D. R., Hubbard, K. & Redmond, K. in Temporal variations in frost-free season in the United States: 1895–2000, *Geophys. Res. Lett.* **31**, 1–4 (2004).
46. FAO. in *Food and Agriculture Oraganization of the United Nations* 218 (2014).
47. U.S. Energy Information Administration. *Electric Sales, Revenue, and Average Price*. Electricity. (https://www.eia.gov/electricity/sales_revenue_price/). (2021). (Accessed 5 March 2021).
48. McCarthy, B. et al. in *Environmental Science and Technology* Vol. 54, 15329–15337 (American Chemical Society, 2020).
49. Zell, W. O. & Sanford, W. E. in *Water Resources Research* Vol. 56, e2019WR026724 (John Wiley & Sons, Ltd, 2020).
50. Yan, L. & Roy, D. P. in *Remote Sensing of Environment* Vol. 172, 67–86 (Elsevier, 2016).
51. National Agricultural Statistics Service (NASS). Surveys: Census of irrigation. U.S. Department of Agriculture. (https://www.nass.usda.gov/Surveys/Guide_to_NASS_Surveys/Farm_and_Ranch_Irrigation/). (2013). (Retrieved March 4, 2021).
52. Mekonnen, M. M. & Hoekstra, A. Y. Four billion people facing severe water scarcity, *Sci. Adv.* **2**, 1500323 (American Association for the Advancement of Science, 2016).
53. Reitz, M., Sanford, W. E., Senay, G. B. & Cazenas, J. Annual estimates of recharge, quick-flow runoff, and evapotranspiration for the contiguous U.S. using empirical regression equations. *Journal of the American Water Resources Association* Vol. 53, 961–983 (Blackwell Publishing Inc., 2017).
54. Zhao, C. et al. in *Proc. National Academy of Sciences of the United States of America* Vol. 114, 9326–9331 (National Academy of Sciences, 2017).
55. Perrone, D. & Jasechko, S. in *Nature Sustainability* Vol. 2, 773–782 (Nature Publishing Group, 2019).
56. Deines, J. M., Kendall, A. D., Butler, J. J. & Hyndman, D. W. in *Environmental Research Letters* Vol. 14, 044014 (IOP Publishing, 2019).
57. Zwickle, A., Feltman, B. C., Brady, A. J., Kendall, A. D. & Hyndman, D. W. in *Environmental Science & Policy* Vol. 124, 517–526 (Elsevier, 2021).
58. Gowda, P. et al. Agriculture and rural communities. Impacts, risks, and adaptation in the United States: Fourth national climate assessment, **2**, 391–437 (2018).
59. Strzepek, K., Yohe, G., Neumann, J. & Boehlert, B. in *Environmental Research Letters* Vol. 5, 044012 (IOP Publishing, 2010).
60. Cooley, D., Maxwell, R. M., & Smith, S. M. Center pivot irrigation systems and where to find them: a deep learning approach to provide inputs to hydrologic and economic models. *Frontiers in Water* **3**, 786016 (2021).
61. Edwards, E. C. & Smith, S. M. in *J. Econ. Hist.* Vol. 78, 1103–1141 (Cambridge University Press, 2018).
62. Perry, E. D., Yu, J. & Tack, J. in Using insurance data to quantify the multidimensional impacts of warming temperatures on yield risk. *Nature Communications* Vol. 11, 1–9 (Nature Publishing Group, 2020).
63. Tack, J., Coble, K. & Barnett, B. in *Agricultural Economics* Vol. 49, 635–647 (John Wiley & Sons, Ltd, 2018).
64. Whitehead, R. L. Ground Water Atlas of the United States: Segment 8, Montana, North Dakota, South Dakota, Wyoming. Report No. 730I, I1-I24 (1996).
65. Foster, T., Gonçalves, I. Z., Campos, I., Neale, C. M. U. & Brozović, N. in *Environmental Research Letters* Vol. 14, 024004 (IOP Publishing, 2019).
66. Hurtt, G. C. et al. in *Geoscientific Model Development* Vol. 13, 5425-5464 (Copernicus GmbH, 2020).
67. Rudnick, D. R. et al. in Deficit irrigation management of maize in the high plains aquifer region: a review. *JAWRA Journal of the American Water Resources Association* Vol. 55, 38–55 (John Wiley & Sons, Ltd, 2019).
68. Lobell, D. et al. Regional differences in the influence of irrigation on climate. *J. Clim.* **22**, 2248–2255 (2009).
69. Pei, L. et al. in Effects of irrigation on summer precipitation over the United States. *J. Clim.* **29** 3541–3558 (2016).
70. Franke, J. A. et al. *Geoscientific Model Development* Vol. 13, 2315–2336 (Copernicus GmbH, 2020).
71. Eyring, V. et al. in *Geoscientific Model Development Discussions* Vol. 8, 10539–10583 (Copernicus GmbH, 2015).
72. Hoogenboom, G. et al. in *Advances in Crop Modelling for a Sustainable Agriculture* 173–216 (Burleigh Dodds Science Publishing, 2019).
73. Jones, C. A., Kiniry, J. R., & Dyke, P. T. CERES-Maize: A simulation model of maize growth and development. (1986).
74. Boote, K. J., Jones, J. W., Hoogenboom, G., & Wilkerson, G. G. Evaluation of the CROPGRO-Soybean model over a wide range of experiments. In *Applications of Systems Approaches at the Field Level: Volume 2 Proceedings of the Second International Symposium on Systems Approaches for Agricultural Development, held at IRRI, Los Baños, Philippines*, 6–8 December 1995 (pp. 113–133). (Springer, Netherlands, 1997).
75. Wilkerson, G., Jones, J., Boote, K., Ingram, K. & Mishoe, J. Modeling soybean growth for crop management. *Trans. ASAE* **26**, 63–0073 (1983).
76. Livneh, B. et al. A spatially comprehensive, hydrometeorological data set for Mexico, the U.S., and Southern Canada 1950–2013. *Sci Data* **2**, 150042 (2015).
77. Livneh, B. et al. A Long-Term Hydrologically Based Dataset of Land Surface Fluxes and States for the Conterminous United States: Update and Extensions. *J. Clim.* **26**, 9384–9392 (2013).
78. Basso, B., Hyndman, D. W., Kendall, A. D., Grace, P. R. & Robertson, G. P. Can Impacts of Climate Change and Agricultural Adaptation Strategies Be Accurately Quantified if Crop Models Are Annually Re-Initialized? *PLOS ONE* **10**, e0127333 (2015).
79. Kiniry, J. R., Ritchie, J. T., Musser, R. L., Flint, E. P. & Iwig, W. C. The Photoperiod Sensitive Interval in Maize1. *Agron. J.* **75**, 687–690 (1983).
80. Jagtap, S. S., & Jones, J. W. Adaptation and evaluation of the CROPGRO-soybean model to predict regional yield and production. *Agric. Ecosyst. Environ.* **93**, 73–85 (2002).
81. Boryan, C., Yang, Z. & Di, L. Deriving 2011 Cultivated Land Cover Data Sets Using USDA National Agricultural Statistics Service Historic Cropland Data Layers. *Proc. of IEEE International Geoscience and Remote Sensing Symposium, July 22-27*, pp. 6297–6300 (Munich, Germany, 2012).
82. Pervez, M. S. & Brown, J. F. Mapping irrigated lands at 250-m scale by merging MODIS data and national agricultural statistics. *Remote Sensing* **2**, 2388–2412 (2010).
83. Lutz, A. F. et al. Selecting representative climate models for climate change impact studies: an advanced envelope-based selection approach. *Int. J. Climatology* **36**, 3988–4005 (2016).
84. Sánchez, E., Romera, R., Gaertner, M. A., Gallardo, C., & Castro, M. A weighting proposal for an ensemble of regional climate models over Europe driven by 1961–2000 ERA40 based on monthly precipitation probability density functions. *Atmos Sci. Lett.* **10**, 241–248 (2009).
85. FAOSTAT, Statistical databases (FAO, Rome, 2019). Accessed 4 March 2021.
86. New, L. Pumping Plant and Irrigation Costs; Texas Agricultural Extension Service: College Station, Texas, 1988.

Acknowledgements

This study was funded by the United States Department of Agriculture National Institute of Food and Agriculture (2018-67003-27406) and National Science Foundation (BCS 1848018). The authors thank Jose R. Lopez for his help running pDSSAT and several reviewers for their thoughtful feedback and suggestions. This paper makes use of agronomic data provided by the United States Department of Agriculture National Agricultural Statistics Service, the Livneh hydrometeorological climate dataset provided by NOAA/OAR/ESRL PSD, Boulder, Colorado, USA. We acknowledge the World Climate Research Program, which, through its Working Group on Coupled Modeling, coordinated and promoted CMIP6. We thank the climate modeling groups for producing and making available their model output, the Earth System Grid Federation (ESGF) for archiving the data and providing access, and the multiple funding agencies who support CMIP6 and ESGF.

Author contributions

T.F.P.: conceptualization, methodology, data curation, formal analysis, writing – original draft, writing – review & editing. J.M.W.: supervision, funding acquisition, conceptualization, methodology. A.D.K.: conceptualization, funding acquisition,

methodology. B.B.: conceptualization, funding acquisition, methodology. L.P.: conceptualization, writing – review & editing. D.W.H: conceptualization, funding acquisition, methodology.

Competing interests

The authors declare no competing interests.

Additional information

Supplementary information The online version contains supplementary material available at https://doi.org/10.1038/s43247-023-00889-0.

Correspondence and requests for materials should be addressed to Trevor Partridge.

Peer review information *Communications Earth & Environment* thanks Lorenzo Rosa and the other, anonymous, reviewer(s) for their contribution to the peer review of this work. Primary Handling Editors: Min-Hui Lo and Heike Langenberg. A peer review file is available

Reprints and permission information is available at http://www.nature.com/reprints

Publisher's note Springer Nature remains neutral with regard to jurisdictional claims in published maps and institutional affiliations.

Open Access This article is licensed under a Creative Commons Attribution 4.0 International License, which permits use, sharing, adaptation, distribution and reproduction in any medium or format, as long as you give appropriate credit to the original author(s) and the source, provide a link to the Creative Commons licence, and indicate if changes were made. The images or other third party material in this article are included in the article's Creative Commons licence, unless indicated otherwise in a credit line to the material. If material is not included in the article's Creative Commons licence and your intended use is not permitted by statutory regulation or exceeds the permitted use, you will need to obtain permission directly from the copyright holder. To view a copy of this licence, visit http://creativecommons.org/licenses/by/4.0/.

This is a U.S. Government work and not under copyright protection in the US; foreign copyright protection may apply 2023